Atmos. Chem. Phys., 23, 1403–1419, 2023
https://doi.org/10.5194/acp-23-1403-2023

Atmospheric Chemistry and Physics
Open Access
EGU

Measurement report: Abundance and fractional solubilities of aerosol metals in urban Hong Kong – insights into factors that control aerosol metal dissolution in an urban site in South China

Junwei Yang[1], Lan Ma[1,2], Xiao He[3], Wing Chi Au[1], Yanhao Miao[1], Wen-Xiong Wang[1,2], and Theodora Nah[1,2]

[1]School of Energy and Environment, City University of Hong Kong, Hong Kong SAR, China
[2]State Key Laboratory of Marine Pollution, City University of Hong Kong, Hong Kong SAR, China
[3]College of Chemistry and Environmental Engineering, Shenzhen University, Shenzhen 518060, China

Correspondence: Theodora Nah (theodora.nah@cityu.edu.hk)

Received: 23 August 2022 – Discussion started: 26 September 2022
Revised: 25 December 2022 – Accepted: 11 January 2023 – Published: 25 January 2023

Abstract. Water-soluble metals are known to produce greater adverse human health outcomes than their water-insoluble forms. Although the concentrations of water-soluble aerosol metals are usually limited by atmospheric processes that convert water-insoluble metals to water-soluble forms, factors that control the solubilities of aerosol metals in different environments remain poorly understood. In this study, we investigated the abundance and fractional solubilities of different metals in size-fractionated aerosols collected at an urban site in Hong Kong and identified the factors that modulated metal solubilities in fine aerosols. The concentrations of total and water-soluble metals in fine and coarse aerosols were the highest during the winter and spring seasons due to the long-range transport of air masses by northerly prevailing winds from emission sources located in continental areas north of Hong Kong. The study-averaged metal fractional solubilities spanned a wide range for both fine (7.8 % to 71.2 %) and coarse (0.4 % to 47.9 %) aerosols, but higher fractional solubilities were typically observed for fine aerosols. Sulfate was found to be strongly associated with both the concentrations of water-soluble Cr, Fe, Co, Cu, Pb, and Mn and their fractional solubilities in fine aerosols, which implied that sulfate-driven acid processing likely played an important role in the dissolution of the water-insoluble forms for these six metals. Further analyses revealed that these strong associations were due to sulfate providing both the acidic environment and liquid water reaction medium needed for the acid dissolution process. Thus, the variability in the concentrations of water-soluble Cr, Fe, Co, Cu, Pb, and Mn and their fractional solubilities were driven by both the aerosol acidity levels and liquid water concentrations, which in turn were controlled by sulfate. These results highlight the roles that sulfate plays in the acid dissolution of metals in fine aerosols in Hong Kong. Our findings will likely also apply to other urban areas in South China, where sulfate is the dominant acidic and hygroscopic component in fine aerosols.

Published by Copernicus Publications on behalf of the European Geosciences Union.

1 Introduction

Chronic exposures to atmospheric aerosols, especially those in the fine mode ($PM_{2.5}$, aerosols with an aerodynamic diameter $\leq 2.5\,\mu m$), have been linked to a myriad of deleterious effects on human health, including morbidity and excess death due to respiratory and cardiovascular diseases (Brook et al., 2010; Cohen et al., 2017). Some of the aerosol chemical species cause a majority of the adverse human health outcomes, even though they comprise a small fraction of the overall aerosol mass (Phalen, 2004; Lippmann, 2014). Metals are ubiquitous chemical species that contribute significantly to airborne aerosol toxicity, although they are typically present in aerosols in trace quantities (Costa and Dreher, 1997; Frampton et al., 1999; Ye et al., 2018; Zhao et al., 2021). Natural sources, especially mineral dust and sea spray, dominate the global sources of aerosol metals (Nriagu, 1989; Garrett, 2000; Deguillaume et al., 2005; Mahowald et al., 2018). However, anthropogenic sources such as industrial activities and vehicular traffic contribute substantial quantities of aerosol metals in urban environments (Garg et al., 2000; Adachi and Tainosho, 2004; Deguillaume et al., 2005; Lough et al., 2005; Birmili et al., 2006; Lee et al., 2007; Cheng et al., 2009; Li et al., 2013; Jiang et al., 2015; Mahowald et al., 2018).

Metals exist in aerosols in water-insoluble and water-soluble forms. Compared with their water-insoluble forms, water-soluble metals have higher bioavailability, which reportedly allows them to produce adverse human health outcomes (Costa and Dreher, 1997; Heal et al., 2009; Fang et al., 2015; D. Gao et al., 2020; He et al., 2021). Some water-soluble transition metal ions (e.g., Fe(II), Fe(III), Cu(I), Cu(II)) are redox-active species and serve as catalysts in reaction cycles (e.g., Fenton-like reactions) to enhance the in vivo production of reactive oxygen species (ROS) (e.g., $\cdot OH$, $HO_2\cdot$, H_2O_2), which subsequently induce the physiological oxidative stress and inflammation involved in a variety of chronic and acute diseases (Bresgen and Eckl, 2015; Lakey et al., 2016; Bates et al., 2019). A recent epidemiologic study reported that water-soluble Fe concentrations in $PM_{2.5}$ showed strong correlations with cardiovascular-related emergency department visits in Atlanta (Ye et al., 2018). Less abundant water-soluble aerosol metals such as Cr and Pb are also known to exhibit both carcinogenic and noncarcinogenic risks to adults and children despite their small quantities (He et al., 2021).

Water-soluble metals also play important roles in ocean biogeochemistry and atmospheric processes. Atmospheric aerosol deposition is an important source of bioavailable dissolved metals in open oceans. The dissolved metals serve as nutrients, and in some cases toxins, for various aquatic species (de Baar et al., 2005; Boyd et al., 2007; Paytan et al., 2009; Jordi et al., 2012). Some transition metal ions such as Fe(III) and Mn(II) ions can facilitate the formation and aging of organic aerosols (Chu et al., 2013, 2017; Al-Abadleh, 2015, 2021; Slikboer et al., 2015), The coupled redox cycling of Cu(I)/Cu(II) and Fe(II)/Fe(III) ions in aerosols has been proposed to be an important mechanism for the uptake of gas-phase HO_2 in aqueous aerosols, which has important implications for the tropospheric OH radical and O_3 budget (Mao et al., 2013, 2017). Mn(II)-catalyzed oxidation of SO_2 on aqueous aerosol surfaces reportedly contributes more than 90 % of the sulfate production during wintertime haze events in China (Wang et al., 2021).

Aerosol metals are primarily emitted into the atmosphere in water-insoluble forms (Nriagu, 1989). While water-soluble aerosol metals can be emitted directly into the atmosphere (Fang et al., 2015), the concentrations of water-soluble aerosol metals are likely limited by atmospheric processes that convert the water-insoluble metal forms to water-soluble forms (Mahowald et al., 2018). Given the important roles that water-soluble aerosol metals play in adverse human health outcomes and atmospheric processes, it is necessary to understand the factors that modulate the atmospheric processing, and hence the solubility, of aerosol metals. Aerosol Fe dissolution has been the focus of most previous studies. A wide range (< 1 % to 98 %) of fractional solubilities (ratio of the water-soluble metal mass concentration to the total metal mass concentration) have been reported for Fe in atmospheric aerosols (Mahowald et al., 2018). Anthropogenic-influenced aerosols generally have higher Fe solubility than fresh mineral dust (Sedwick et al., 2007; Schroth et al., 2009; Oakes et al., 2012). However, Fe solubility varies substantially in aerosols in different urban environments with high levels of anthropogenic activity, e.g., 1 % to 12 % in four cities in East China (Zhu et al., 2020) vs. around 20 % to 50 % in Hong Kong, South China (Jiang et al., 2014, 2015). Although there are a number of atmospheric processes that can influence aerosol metal solubilities, acid processing and the formation of stable Fe–organic complexes are two key chemical processes known to enhance aerosol Fe dissolution (Deguillaume et al., 2005; Ingall et al., 2018; Tao and Murphy, 2019; Giorio et al., 2022). At present, it remains difficult to explain the variability in aerosol Fe solubility in urban environments, as the extent to which aerosol Fe dissolution is controlled by factors such as aerosol acidity and/or the presence of organic ligands (e.g., oxalate) in different urban environments is still not well understood. Even less is known about the factors that control the solubilities of other aerosol metals beyond Fe.

Hong Kong is a highly developed, densely populated city in the Guangdong–Hong Kong–Macau Great Bay Area (GBA) urban agglomeration, which is a large business and economic hub located in the southern part of China. While there have been some studies on the fractional solubilities of various aerosol metals in Hong Kong (Jiang et al., 2014, 2015), to the best of our knowledge, there has not been a study that has investigated the factors that control the solubilities of aerosol metals in Hong Kong. In this study, we investigated the abundance and fractional solubilities of

10 metals (Fe, Cu, Al, V, Cr, Mn, Co, Ni, Cd, and Pb) in aerosols at an urban site in Hong Kong. Our main goal is to identify the key factors that control the solubilities of metals in fine aerosols, as they are believed to exert higher toxicity than coarse aerosols due to their small sizes. We focus primarily on aerosol metal dissolution through the acid processing and/or metal–organic complexation mechanisms. Hence, other aerosol species were also measured for comparisons to total and water-soluble metals. The measured aerosol inorganic ion composition was used as input for a thermodynamic model to determine the aerosol acidity levels, liquid water concentrations, and pH.

2 Methods

2.1 Ambient sampling

The sampling campaign took place at ground level next to a road in Kowloon Tong (22.3367° N, 114.1724° E). Kowloon Tong is located in the southern side of Hong Kong, and it is primarily a residential and commercial district which is close to Mongkok, one of the busiest commercial and most densely populated areas in Hong Kong with high-density traffic flow. Weekly size-fractionated aerosol samples were collected from 7 March to 4 April 2021 (spring season), from 23 to 30 June 2021 and from 7 to 14 July 2021 (summer season), from 13 September to 11 October 2021 (fall season), and from 15 December 2021 to 26 January 2022 (winter season). Back-trajectory calculations carried out with the Hybrid Single-Particle Lagrangian Integrated Trajectory (HYSPLIT) model using meteorological data from the NCEP/NCAR Reanalysis (2.5° latitude–longitude grid) showed that the sampling site was under the influence of continental and marine air masses during the sampling periods, although the contributions of these air masses varied with season (Fig. S1 in the Supplement).

An 11-stage microorifice uniform deposit impactor (MOUDI; model 110, MSP Corp., USA) was used to collect and divide aerosols into different aerosol size bins under ambient conditions. Aerosols were collected on prebaked 47 mm diameter quartz filters (Tissuquartz 2500QAT-UP, Pall Corp., USA). The nominal cut points for the 11 MOUDI impactor stages were 0.056, 0.1, 0.18, 0.32, 0.56, 1.0, 1.8, 3.2, 5.6, 10, and 18 µm. In the discussion below, for simplicity, we refer to aerosols collected on impactor stages with nominal cut points of 0.056, 0.1, 0.18, 0.32, 0.56, 1.0, and 1.8 µm as "fine aerosols", whereas aerosols collected on impactor stages with nominal cut points of 3.2, 5.6, 10, and 18 µm are referred to as "coarse aerosols". Aerosols were collected continuously for 7 d (i.e., 24 h × 7 d). This resulted in 4-, 2-, 4-, and 6-weekly sets of aerosol filter samples collected during the spring, summer, fall, and winter seasons, respectively. After collection, the aerosol filter samples were immediately extracted for chemical analysis.

Thermodynamic model calculations used to determine the aerosol acidity levels, liquid water concentrations, and pH (Sect. 2.3) require gas-phase NH_3 concentrations, ambient temperature, and relative humidity (RH) as model input. Hence, weekly NH_3 measurements were performed during each sampling period using four passive sampling devices (PSDs) and pre-coated collection pads (PS-100 and PS-154, Ogawa & Co., Ltd., Pompano Beach, FL), except from 7 to 28 March 2021. The exposed PSD collection pads were extracted in purified deionized water (18.2 MΩ cm) using the protocol recommended by the manufacturer. These aqueous extracts were subsequently analyzed by ion chromatography (Sect. 2.2) to determine the average NH_3 concentration during the sampling period. A Vantage Vue weather station (model 6250, Davis Instruments, USA) was used to measure ambient temperature and RH during each sampling period.

2.2 Chemical analysis

Each aerosol filter sample was cut into four equal pieces for chemical analysis of different chemical components. One of the four pieces was extracted in purified deionized water via sonication (1 h), followed by high-speed vortexing at 3000 rpm (15 min). The resulting aqueous extract was filtered using 0.22 µm pore size nylon filters (Tianjin Jinteng Experiment Equipment Co., Ltd., Tianjin, China) before it was analyzed by a total organic carbon (TOC) analyzer (TOC-VCSH, Shimadzu Corporation, Japan) to determine the concentration of water-soluble organic carbon (WSOC). The TOC analyzer has a limit of detection (LOD) of 0.5 mg L^{-1}. The second filter piece was similarly extracted in purified deionized water via sonication (1 h) and high-speed vortexing at 3000 rpm (15 min), and it was filtered using 0.22 µm pore size nylon filters before it was analyzed by an ion chromatography (IC) system (Dionex ICS-1100, ThermoFisher Scientific, USA) using an isocratic method to determine the concentrations of water-soluble anions (NO_3^-, SO_4^{2-}, Cl^-, and $C_2O_4^{2-}$) and cations (NH_4^+, Na^+, K^+, Ca^{2+}, and Mg^{2+}). Anion separation was achieved using a 4 mm × 250 mm anion exchange column (Dionex IonPac AS18, ThermoFisher Scientific, USA) equipped with a 4 mm × 50 mm guard column (Dionex IonPac AG18, ThermoFisher Scientific, USA). Cation separation was achieved using a 4 mm × 250 mm cation exchange column (Dionex IonPac CS12A, ThermoFisher Scientific, USA) equipped with a 4 mm × 50 mm guard column (Dionex IonPac CG12A, ThermoFisher Scientific, USA). Solutions of 16 mM potassium hydroxide and 31 mM methanesulfonic acid were used as eluents at a flow rate of 1.0 mL min^{-1} for the anion and cation separations, respectively. The cation IC method was also used to analyze the aqueous extracts from the exposed PSD collection pads to determine the average NH_3 concentration during each sampling week. The LODs for the cation IC method were 0.025 mg L^{-1} for NH_4^+, Na^+, and Mg^{2+}, and 0.025 mg L^{-1} for K^+ and Ca^{2+}. The LODs

for the anion IC method were 0.125 mg L^{-1} for NO_3^-, SO_4^{2-}, and $C_2O_4^{2-}$, and 0.025 mg L^{-1} for Cl^-.

The remaining two filter pieces were used for metal analysis. One filter piece was extracted with purified deionized water in metal-free centrifuge tubes via sonication (1 h), followed by high-speed vortexing at 3000 rpm (15 min). The resulting aqueous extract was filtered using 0.22 µm pore size nylon filters and was then acidified with 2 % HNO_3 prior to storage at 4 °C before chemical analysis of water-soluble metals. The filterable metal fraction in the water extracts, defined in this study as water-soluble metals, will include all dissolved metal forms and any colloidal particles with diameters smaller than 0.22 µm. This assumes that all colloidal particles with diameters smaller than 0.22 µm can penetrate through the syringe filter and that the syringe filter's retention efficiency of particles with diameters larger than 0.22 µm is 100 %. The exact sizes and distribution of metal colloidal particles in the filterable metal fraction in water extracts in this study are not known. However, Yang et al. (2021) recently reported that around 84 % of Fe and Cu colloidal particles that penetrated through 0.45 µm syringe filters had nominal diameters smaller than 4 nm. The remaining 16 % of Fe and Cu colloidal particles had nominal diameters between 4 nm and 0.45 µm and may be in water-insoluble forms (e.g., Fe and Cu oxides), so they may not be "true" water-soluble species. Hence, analogous to observations made by Yang et al. (2021), it is possible that the filterable metal fractions in water extracts in this study contain some metals in water-insoluble forms with diameters smaller than 0.22 µm that penetrated through the 0.22 µm pore size filters. The last filter piece was extracted via acid digestion for chemical analysis of total metals. The acid digestion protocol that we employed was adapted from published protocols (Jiang et al., 2014, 2015). The filter piece was extracted in an acid digestion matrix (16 N HNO_3 and 12 N HCl at a 3 : 1 volume ratio) placed in a glass microwave vial using a microwave synthesizer (Initiator+, Biotage, Sweden). The microwave synthesizer's digestion temperature was ramped up to 150°C and then held for 15 min. This was followed by cooling and ventilation for 30 min. An evaporation and recovery treatment was performed next in order to remove Cl^- from the matrix to reduce its interference during chemical analysis. The digestion solution was heated to 200°C on a hot plate. Once the solution was observed to be almost dry, 16 N HNO_3 was added. When the solution was observed to be almost dry the second time, 2 % HNO_3 was added. The resulting solution was filtered using 0.22 µm pore size nylon filters and then stored at 4 °C before chemical analysis of total metals. A standard reference material of San Joaquin soil (SRM 2709a, NIST) was digested and analyzed using the same protocols to evaluate the metal recoveries. Recoveries of 59.4 % for Cr, 67.0 % for Al, 93.7 % for Fe, 93.6 % for Ni, 100.2 % for Co, 98.6 % for Pb, 95.8 % for Cu, 99.6 % for Mn, 70.5 % for V, and 94.3 % for Cd were observed.

The concentrations of 10 water-soluble and total metals (^{27}Al, ^{51}V, ^{52}Cr, ^{55}Mn, ^{57}Fe, ^{59}Co, ^{60}Ni, ^{65}Cu, ^{111}Cd, and ^{208}Pb) were determined by an inductively coupled plasma mass spectrometry (ICP–MS) instrument (NexION 1000, PerkinElmer Inc., USA). The following parameters were used for the ICP-MS instrument: 0.98 L min^{-1} nebulizer gas flow, 1.2 L min^{-1} auxiliary gas flow, 15 L min^{-1} plasma gas flow, 5 mL min^{-1} He gas flow, 1600 W radio frequency (RF) power, 35 rpm nebulizer pump rate, and 35 rpm sample pump rate. A multielement calibration standard (IV-STOCK-13, Inorganic Ventures, USA) was used to quantify the 10 water-soluble and total metals. An internal standard solution of ^{115}In (10 µg L^{-1}) was added to all samples and standards to monitor analytical drift. The LODs for ^{27}Al, ^{51}V, ^{52}Cr, ^{55}Mn, ^{57}Fe, ^{59}Co, ^{60}Ni, ^{65}Cu, ^{111}Cd, and ^{208}Pb were 87, 0.8, 2.8, 1.6, 277, 0.7, 4.6, 6.7, 1, and 0.4 ng L^{-1}, respectively. To identify the major sources of the aerosol metals, source apportionment was performed with positive matrix factorization (PMF) (Paatero and Tapper, 1994; Paatero, 1997) using the aerosol chemical components measured by the ICP-MS and IC. Details of the PMF method used can be found in Sect. S1 in the Supplement (SI).

2.3 Thermodynamic modeling

The thermodynamic model ISORROPIA II was used to determine aerosol acidity levels, liquid water concentrations, and pH (Fountoukis and Nenes, 2007). Similar to the methodology employed by Fang et al. (2017), we ran ISORROPIA II for each of the MOUDI impactor stages that collected fine aerosols. The measured water-soluble NH_4^+, SO_4^{2-}, NO_3^-, Cl^-, Na^+, Ca^{2+}, K^+, and Mg^{2+} ions for the aerosols collected on the MOUDI impactor stage, gas-phase NH_3, ambient temperature, and RH were used as model input. As gas-phase NH_3 measurements were not available from 7 to 28 March 2021, we used NH_3 measurements from 28 March to 4 April 2021 as model input for the spring calculations. The measured NH_3 concentrations during the study ranged from 3.60 to 8.18 µg m^{-3}, with a study-averaged concentration of 5.01 ± 1.25 µg m^{-3}. ISORROPIA II was run in "forward" mode and under the assumption that the aerosols existed in a "metastable" equilibrium state (i.e., the aerosols only existed in liquid form). These calculations assumed that the aerosols were in thermodynamic equilibrium with the gas phase. While fine aerosols satisfy this equilibrium condition, equilibrium between the gas and aerosol phases of coarse aerosols cannot be achieved due to kinetic limitations (Fountoukis et al., 2009). Thus, aerosol pH values were not calculated for coarse aerosols.

Fine-aerosol pH values were calculated based on the molal definition (Pye et al., 2020):

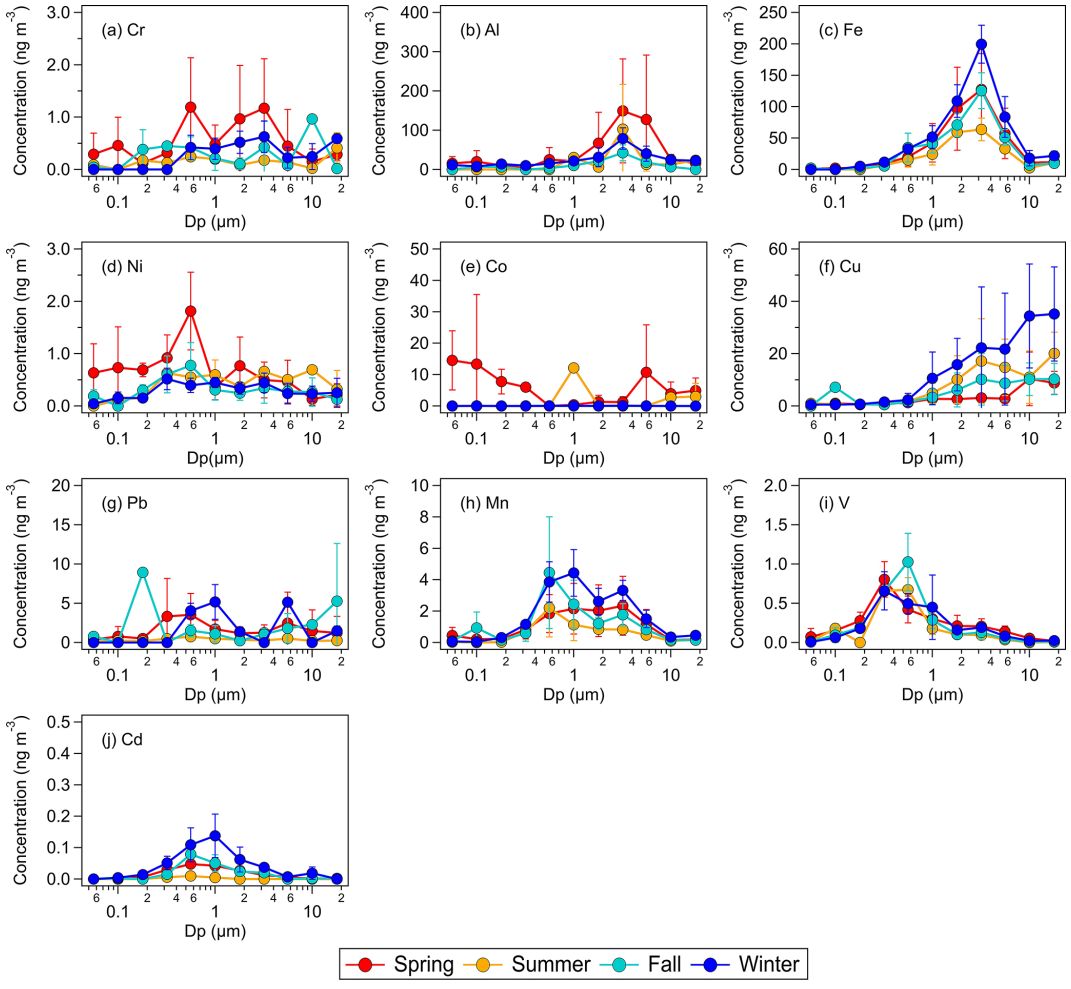

Figure 1. Seasonal average concentrations of total elemental metals in size-fractionated aerosols sampled by the MOUDI with the following nominal cut points (Dp): 0.056 µm (size fraction 1), 0.1 µm (size fraction 2), 0.18 µm (size fraction 3), 0.32 µm (size fraction 4), 0.56 µm (size fraction 5), 1.0 µm (size fraction 6), 1.8 µm (size fraction 7), 3.2 µm (size fraction 8), 5.6 µm (size fraction 9), 10 µm (size fraction 10), and 18 µm (size fraction 11). The error bars represent 1 standard deviation of the seasonal average value.

$$\mathrm{pH} = -\log_{10}\gamma_{\mathrm{H^+H^+_{aq}}} = -\log_{10}\frac{1000\mathrm{H^+_{air}}}{W_i + W_o}$$
$$\cong -\log_{10}\frac{1000\mathrm{H_{air}}^+}{W_i}, \quad (1)$$

where $\gamma_{\mathrm{H^+}}$ is the hydronium ion activity coefficient, $\mathrm{H^+_{aq}}$ is the hydronium ion concentration within the ambient aerosol liquid water (mol $\mathrm{L^{-1}}$), $\mathrm{H^+_{air}}$ is the hydronium ion concentration per volume of air (µg $\mathrm{m^{-3}}$), and W_i and W_o are the aerosol liquid water concentrations (µg $\mathrm{m^{-3}}$) associated with inorganic and organic species, respectively. $\mathrm{H^+_{air}}$ and W_i are the output provided by the ISORROPIA II model, which assumes that $\gamma_{\mathrm{H^+}}$ is equal to unity. W_o can be estimated from the WSOC measurements using the approach described in Sect. S2. WSOC concentrations in the size-fractionated aerosols ranged from 0 to 4.6 µg $\mathrm{m^{-3}}$. The inclusion of W_o into calculations did not impact aerosol pH significantly (Fig. S2). Thus, only aerosol pH values calculated using W_i will be reported here. Similar to Fang et al. (2017), lower pH values were typically calculated for aerosols collected on MOUDI impactor stages with smaller nominal cut points (i.e., these aerosols had smaller aerodynamic aerosol diameters) due to the higher mass concentrations of sulfate in these smaller aerosols. The fine aerosols were mostly acidic, with about 74 % of the calculated pH values lying between 2 and 4.

3 Results and discussion

3.1 Total metals

Figure 1 shows the seasonal average mass concentrations of the 10 measured total metals in size-fractionated aerosols. The size distributions of five of the metals (Al, Fe, Mn, V, and Cd) consistently exhibited a single mode. The modes

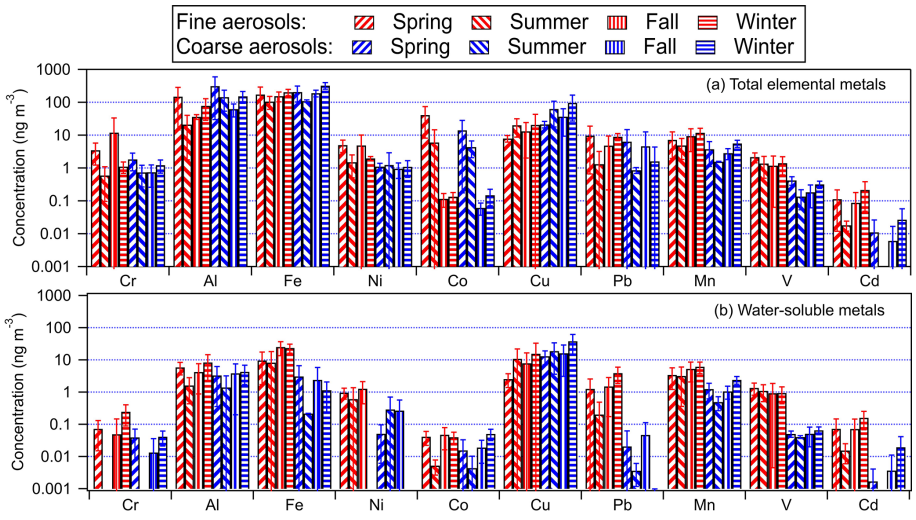

Figure 2. Seasonal average mass concentrations of **(a)** total metals and **(b)** water-soluble metals in fine (red) and coarse (blue) aerosols. The error bars represent 1 standard deviation. The y axes are on logarithmic scales.

for Mn, V, and Cd were predominantly found in the fine mode, whereas the modes for Fe and Al were predominantly found in the coarse-aerosol mode. Figure 2a shows the seasonal average concentrations of the 10 measured total metals in fine and coarse aerosols. For most of the metals, higher mass concentrations were measured during the winter and/or spring seasons. This could be attributed to the long-range transport of polluted air masses by northerly prevailing winds from emission sources located in continental areas north of Hong Kong (Fig. S1). The metals could be arranged in the following order based on their abundances: Fe > Al > Cu > Co > Mn > Pb > Cr > Ni > V > Cd. This order of abundance was the same for both fine and coarse aerosols.

The mass concentrations of the two most abundant metals, Fe and Al, were usually higher than 10 ng m^{-3} in both fine and coarse aerosols. Fe, Al, and Cu had substantially higher mass concentrations in coarse aerosols than in fine aerosols. The positive correlations of the mass concentrations of Al with the mass concentrations of Fe and Cu were the strongest among the nine metals ($R = 0.62$ and $R = 0.52$, respectively) and were statistically significant (Fig. S3), which could be explained by large mass concentrations of Al, Fe, and Cu originating from similar sources. These three metals are known to originate mainly from dust sources (e.g., mineral dust and road dust) (Hopke et al., 1980; Garg et al., 2000; Adachi and Tainosho, 2004; Lough et al., 2005; Chow et al., 2022). This is consistent with results from our PMF source apportionment analysis, which showed that the "dust" factor had large mass contributions from Al, Fe, and Cu (Figs. S4, S5). Mn, Ni, V, and Cd had higher mass concentrations in fine aerosols than in coarse aerosols. These four metals are known to be consistently found in aerosols from anthropogenic sources such as vehicle and ship emissions as well as combustion and industrial processes (Chow et al., 2022). Pb, Cr, and Co had mostly similar concentrations in the fine and coarse aerosols. Interestingly, the mass concentrations of Mn and Cr were positively correlated with the mass concentration of Al ($R = 0.42$ and $R = 0.33$, respectively), and these correlations were statistically significant (Fig. S3). Our PMF analysis apportioned Al to two factors, "dust" and "industrial factor 1", although the Al contribution to "industrial factor 1" was substantially smaller compared with "dust" (Figs. S4, S5). The "dust" factor had a significant Mn contribution, which could explain the strong correlation between the mass concentrations of Al and Mn. Cr was primarily apportioned to "industrial factor 1", which could explain the strong correlation between the mass concentrations of Al and Cr. The mass concentrations of Ni, V, Cd, Pb, and Co showed weak correlations with the mass concentration of Al (Fig. S3).

Jiang et al. (2015) previously measured the mass concentrations of various total metals in $PM_{2.5}$ and $PM_{2.5–10}$ in Kowloon Tong. The authors carried out their measurements from 12 November to 10 December 2012 (winter) and from 8 April to 13 May 2013 (spring/summer). To gain some insights into how the aerosol metal concentrations at this urban site have changed since 2012–2013, we compared the average mass concentrations of total metals in fine and coarse aerosols measured in this study to those measured by Jiang et al. (2015). As shown in Table S1 in the Supplement, lower mass concentrations were measured in fine (21 % to 93 % lower) and coarse (0.5 % to 92 % lower) aerosols for most of the metals in this study. While the lower aerosol metal mass concentrations could be partly attributed to lower levels of anthropogenic activities in 2021–2022 due to COVID-19, it is likely that the implementation of numerous local and regional air pollution policies to reduce industrial and

transport-related emissions over the last decade contributed largely to this decrease. For instance, industrial upgrades resulting from the implementation of the "double transfer" policy (industry and labor transfer away from primary industries) in Guangdong likely caused the decline in the mass concentrations of metals that are typically associated with industrial activities, such as Cu and Mn (Zhong et al., 2013; Chow et al., 2022). In addition, government policies driving the switch to cleaner fuels for energy generation and transport in Hong Kong and the GBA likely caused the decline in the mass concentrations of metals such as Pb, Ni, V, and Fe. Interestingly, higher mass concentrations were measured for Fe and Cu in coarse aerosols in this study compared with those measured by Jiang et al. (2015). Fe and Cu in coarse aerosols have previously been linked to resuspended road dust from brake and tire wear (Garg et al., 2000; Adachi and Tainosho, 2004; Lough et al., 2005). Based on publicly available government data (https://www.td.gov.hk, last access: 23 May 2022), the number of registered motor vehicles in Hong Kong has increased by about 34 % over the last decade. It is possible that the higher Fe and Cu mass concentrations in coarse aerosols in this study were due to increased contributions from road dust as a result of the increased vehicle fleet size at the urban site.

A PMF source apportionment analysis was performed to determine the major sources of aerosol metals measured in this study (Sect. S1). A five-factor solution was selected because it gave the most reasonable factor profiles and had high stability. The five factors were broadly classified as "sea salt", "dust", "ship emissions", "industrial factor 1", and "industrial factor 2" based on the tracer species with the highest mass loadings in each factor (Fig. S4). A discussion on how these five factors were classified can be found in Sect. S1. Figure S5 shows the seasonal mass contributions of each source to each metal species in coarse and fine aerosols. Metals with large fractions in the dust and sea salt source factor profiles generally had higher mass concentrations in coarse aerosols. Conversely, metals with large fractions in the ship emissions and industrial source factor profiles generally had higher mass concentrations in fine aerosols. Higher mass contributions were usually observed in the winter and/or spring seasons, which could be attributed to the long-range transport of polluted air masses by northerly prevailing winds from emission sources located in continental areas north of Hong Kong (Fig. S1).

3.2 Water-soluble metals

Figure 3 shows the seasonal average mass concentrations of water-soluble metals in size-fractionated aerosols. The size distribution of six of the water-soluble metals (Cr, Fe, Pb, Mn, V, and Cd) mostly exhibited a single mode, all of which were found in the fine aerosol mode. Fe, Mn, V, and Cd exhibited a single mode for both their total and water-soluble components (Figs. 1, 3). Of these four metals, only the modes of total and water-soluble Fe showed obvious differences, with total Fe exhibiting a mode at around 3.2 µm (size fraction 8) and water-soluble Fe exhibiting a mode at around 0.56–1.0 µm (size fractions 5–6). The modes of total and water-soluble Cu also showed obvious differences. While the mode of total Cu was at $\geq$ 18 µm (Fig. 1f), the modes of water-soluble Cu were found at substantially small aerosol sizes (Fig. 3f).

Figure 2b shows the seasonal average mass concentrations of water-soluble metals in fine and coarse aerosols. Similar to the total metals, higher mass concentrations of water-soluble metals were usually measured during the winter and/or spring seasons. With the exception of Cu, the water-soluble metals usually had higher mass concentrations in fine aerosols than in coarse aerosols. The water-soluble metals generally had the same order of abundance as the total metals with some slight variations. The mass concentrations of water-soluble metals generally correlated with the mass concentrations of total metals (Table S2). This indicated that the water-soluble metals were largely derived from their total metals through atmospheric processing, and/or that water-soluble and water-insoluble metals have the same emission sources. For most of the metals, correlations between the mass concentrations of water-soluble and total metals were higher for fine aerosols than for coarse aerosols. This could be due to enhanced metal dissolution in fine aerosols via acid processing and/or the formation of stable metal–organic complexes, which are two atmospheric chemical processes that play key roles in influencing the solubilities of aerosol metals at many locations. This is because acidic inorganic species that promote acid processing and organic species that can serve as organic ligands are typically present in larger quantities in fine aerosols than in coarse aerosols. It is also possible that differences in metal mineralogy and atmospheric processing mechanisms in fine vs. coarse aerosols could have contributed to differences in the metal dissolution rates (Oakes et al., 2012; Longo et al., 2016; Ingall et al., 2018).

Figure 4 shows the study-averaged fractional solubilities for the 10 metals in fine and coarse aerosols. The study-averaged metal fractional solubilities spanned a wide range for both fine (7.8 % to 71.2 %) and coarse (0.4 % to 47.9 %) aerosols. With the exception of Cu, the metals generally exhibited higher fractional solubilities in fine aerosols compared with coarse aerosols. The aerosol size-dependent metal fractional solubility could be explained by differences in the aerosol composition and metal mineralogy, which resulted in different metal dissolution rates and/or mechanisms for aerosols of different sizes. Our observations of mostly higher metal fractional solubilities in fine aerosols are consistent with previous studies conducted in Hong Kong and other locations worldwide (Baker et al., 2006, 2020; Jiang et al., 2014, 2015; Fang et al., 2017; Y. Gao et al., 2019, 2020; Zhang et al., 2022). No season-dependent trend was observed for the metal fractional solubilities.

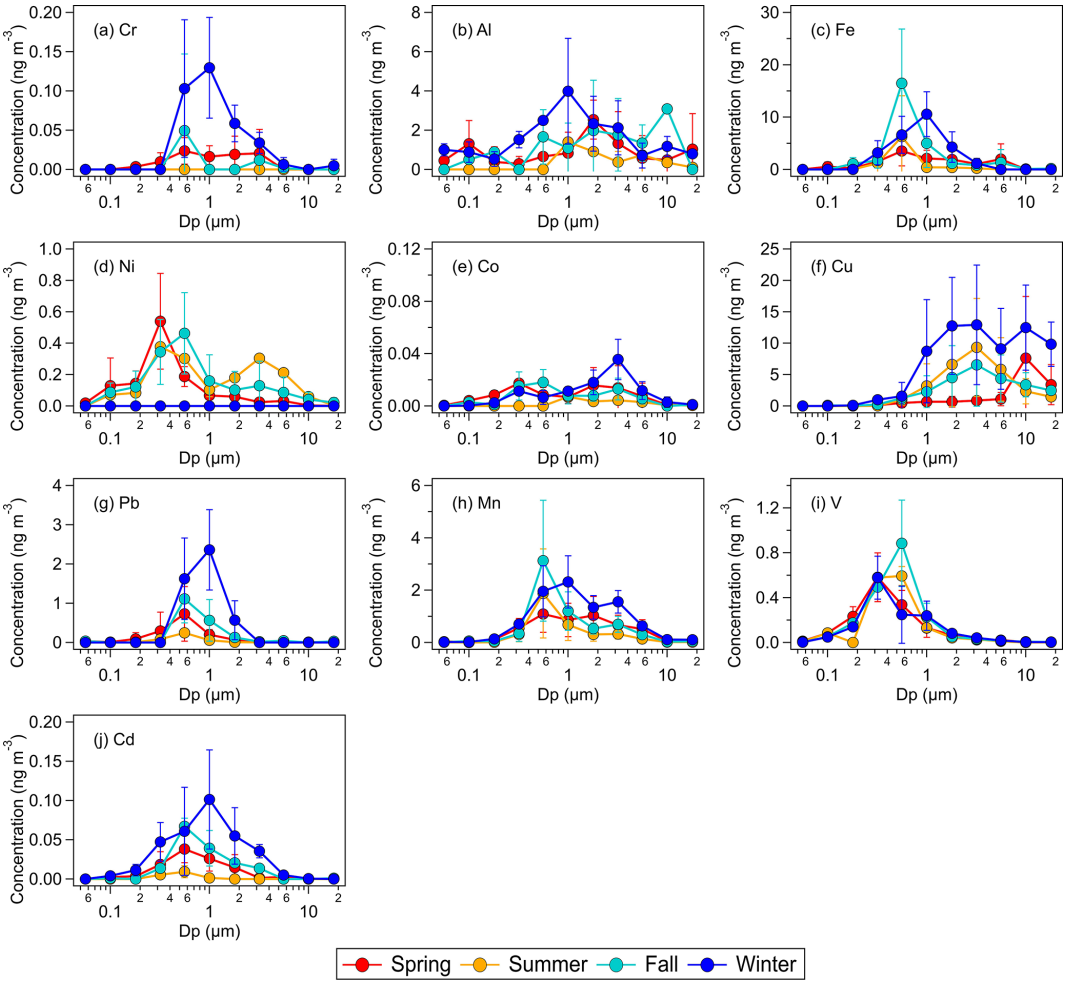

Figure 3. Seasonal average concentrations of water-soluble metals in size-fractionated aerosols sampled by the MOUDI with the following nominal cut points (Dp): 0.056 µm (size fraction 1), 0.1 µm (size fraction 2), 0.18 µm (size fraction 3), 0.32 µm (size fraction 4), 0.56 µm (size fraction 5), 1.0 µm (size fraction 6), 1.8 µm (size fraction 7), 3.2 µm (size fraction 8), 5.6 µm (size fraction 9), 10 µm (size fraction 10), and 18 µm (size fraction 11). The error bars represent 1 standard deviation of the seasonal average value.

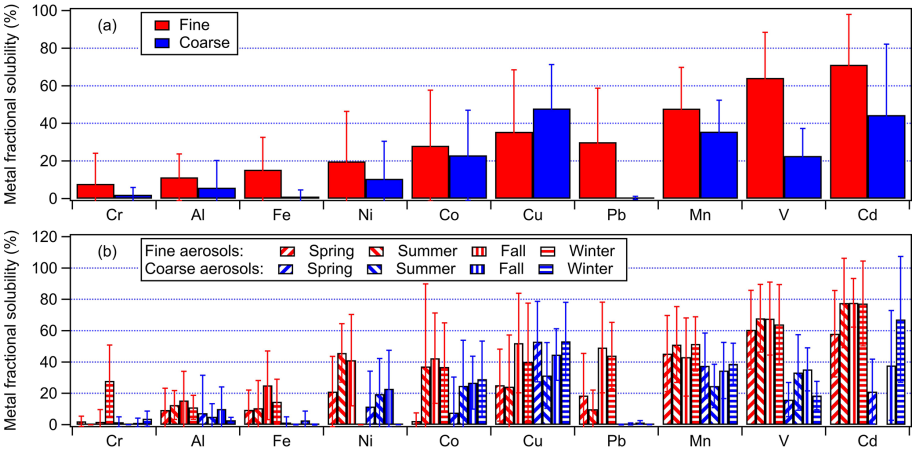

Figure 4. **(a)** Study-averaged fractional solubilities of metals in fine and coarse aerosols. **(b)** Seasonal average fractional solubilities of metals in fine and coarse aerosols. The error bars represent 1 standard deviation.

Some studies have reported that aerosol metal fractional solubilities will exhibit inverse relationships with the total metal concentrations as a result of atmospheric processing (Baker and Jickells, 2006; Sholkovitz et al., 2012; Mahowald et al., 2018; Shelley et al., 2018; Zhang et al., 2022). There was significant scatter in many of our datasets (Fig. S6), which made it difficult to discern some of the relationships between the metal fractional solubilities and total metal concentrations. Inverse relationships between the fractional solubility and total metal concentration were noticeable for Cr, Al, Fe, Ni, Cu, Pb, and Mn. However, inverse relationships between the Co, V, and Cd fractional solubilities and their total metal concentrations were less noticeable due to their low concentrations and scatter in their datasets. A number of factors could have contributed to the scatter in the datasets. For instance, the scatter could be a result of the total and water-soluble metal concentrations being substantially different in individual aerosol particles, which would not be captured by the bulk chemical analysis performed in this study (Oakes et al., 2012; Longo et al., 2016; Ingall et al., 2018). The metal dissolution rates in individual aerosol particles could also be significantly different due to differences in metal mineralogy, aerosol acidity levels, presence of organic ligands, etc. in individual aerosol particles.

3.3 Factors that control the aerosol metal solubilities

Here, we identify the factors that control metal solubilities in fine aerosols, as they are believed to exert higher toxicity than coarse aerosols due to their small sizes. Our analyses focus on aerosol metal dissolution via metal–organic complexation reactions and acid processing, which are two atmospheric chemical processes believed to drive aerosol metal dissolution in most environments. Laboratory studies have shown that the presence of organic ligands enhances Fe dissolution in aerosols (Paris et al., 2011; Chen and Grassian, 2013; Paris and Desboeufs, 2013; Wang et al., 2017). Water-soluble dicarboxylic acids, especially oxalate, form stable complexes with Fe ions, which will lower the energy barrier for Fe dissolution. While evidence of organic ligand-promoted metal dissolution in ambient aerosols has been less conclusive, recent field studies compared the oxalate and water-soluble Fe concentrations to show that the presence of organic ligands could contribute to aerosol Fe solubility. For instance, strong positive correlations between oxalate and water-soluble Fe mass concentrations were observed for $PM_{2.5}$ collected at six urban and rural sites in Canada (Tao and Murphy, 2019). The Fe fractional solubility was also observed to be positively correlated with the molar ratio of oxalate and Fe for $PM_{2.5}$ collected at a suburban site in Qingdao, China (Zhang et al., 2022).

To investigate whether organic ligands influenced aerosol metal solubilities in this study, we attempted to measure oxalate in the size-fractionated aerosol samples using IC. However, we could not detect oxalate, which indicated that the concentrations of oxalate (if present) were below the detection limits of our IC instrument. It should be noted that, although a recent study reported the copresence of Fe and oxalate in individual aerosol particles at a suburban site in Hong Kong using single-particle mass spectrometry (Zhou et al., 2020), organic ligand-promoted metal dissolution is a slow process, and it plays a minor role in metal dissolution under low-pH conditions (Zhu et al., 1993). The fine aerosols collected in this study were mostly acidic, with about 60 % of the calculated pH values being less than 3. This suggested that organic ligand-promoted dissolution may have played a minor role in enhancing aerosol metal solubilities in this study due to the acidic nature of the aerosols.

The acidic nature of the aerosols raises the possibility that acid processing played a major role in enhancing aerosol metal solubilities. A previous study that utilized nanoscale single-particle mass spectrometric and imaging techniques to analyze the mixing states of Fe-containing aerosols collected over the East China Sea provided insights into the mechanism of Fe dissolution by acidic species that condensed onto atmospheric aerosols (Li et al., 2017). The authors reported that Fe oxide-rich aerosols emitted from steel plants and coal combustion were coated with thick layers of acidic sulfate after 1 to 2 d of atmospheric aging. These sulfate coatings originated from the condensation of sulfuric acid, which was formed from reactions of anthropogenic SO_2. While the fresh aerosols were composed primarily of insoluble Fe oxide, the aged aerosols contained soluble Fe sulfate that was internally mixed in the sulfate coatings. Although the mechanism proposed by Li et al. (2017) focused on explaining how sulfate-driven acid processing leads to the dissolution of the water-insoluble forms of Fe, this mechanism likely applies to the other aerosol metals as well. During acid processing, acidic species have to overcome the buffering capacity of the aqueous aerosol particle to raise the aerosol acidity level to the point where the dissolution of metal species is thermodynamically favored. Sulfate was the most abundant aqueous-phase acidic species in our size-fractionated aerosol samples. The concentrations of nitrate (another aqueous-phase acidic species) were very low (about 18 times lower than sulfate, on average), while aqueous-phase organic acids were not detected. Hence, we first analyzed the relationships between the concentrations of water-soluble metals and sulfate. Figure 5 shows that, despite the scatter in the datasets, the concentrations of water-soluble metals were positively correlated with the concentration of sulfate, although the correlations between the concentrations of sulfate and water-soluble Al and Ni were not statistically significant. These positive correlations could be due, in part, to the water-soluble metals and sulfate precursor (i.e., SO_2) being emitted from the same sources. However, the masses of primary water-soluble aerosol metals are not known. The positive correlations could also be due to the role that sulfate plays in aerosol metal dissolution during acid processing.

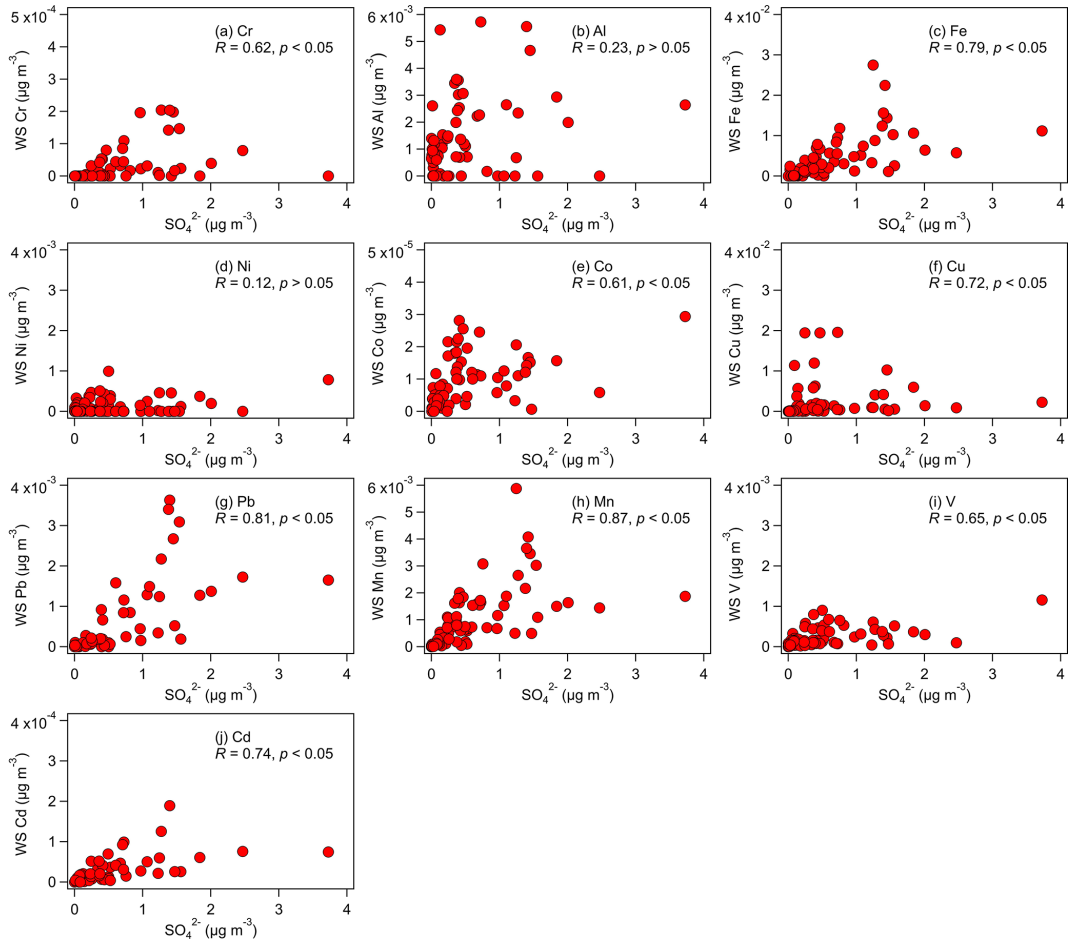

Figure 5. Relationships between the mass concentrations of water-soluble (WS) metals and sulfate in fine aerosols. Only data with nonzero total metal concentrations were used in the figures. Also shown are the Spearman correlation coefficients for each relationship.

Table 1. Spearman rank correlations of the metal fractional solubilities with W_i and H^+_{air} in fine aerosols.

Metal	Sulfate	W_i	H^+_{air}	pH
Cr	**0.62**	**0.42**	**0.48**	−0.16
Al	0.14	0.08	0.14	−0.06
Fe	**0.53**	**0.31**	**0.50**	**–0.33**
Ni	0.03	0.01	0.18	**–0.26**
Co	**0.41**	**0.41**	**0.23**	−0.05
Cu	**0.74**	**0.72**	**0.24**	−0.07
Pb	**0.53**	**0.41**	**0.34**	−0.13
Mn	**0.49**	**0.43**	**0.23**	−0.01
V	0.14	0.01	0.21	−0.20
Cd	0.04	0.10	0.13	0.22

Bold values are statistically significant ($p < 0.05$).

To investigate the roles that sulfate and nitrate played in controlling aerosol metal solubilities, we analyzed the relationships between the metal fractional solubilities and sulfate and nitrate concentrations. In general, the correlations between the metal fractional solubilities and sulfate concentration (Table 1) were substantially higher than the correlations between the metal fractional solubilities and nitrate concentration (Table S3). This implied that sulfate likely plays a more important role than nitrate in controlling aerosol metal solubilities, which is not surprising given the low concentrations of nitrate detected (about 18 times lower than sulfate, on average). Analyses of the correlations between the metal fractional solubilities and sulfate concentration (Table 1, Fig. 6) indicated that the Cr, Fe, Co, Cu, Pb, and Mn fractional solubilities were positively correlated with the sulfate concentration, and these correlations were statistically significant. This implied that sulfate played a key role in the formation of water-soluble Cr, Fe, Co, Cu, Pb, and Mn, likely though sulfate-driven acid dissolution of their water-insoluble forms. Conversely, the positive correlations between the sulfate concentration and the Al, Ni, V, and

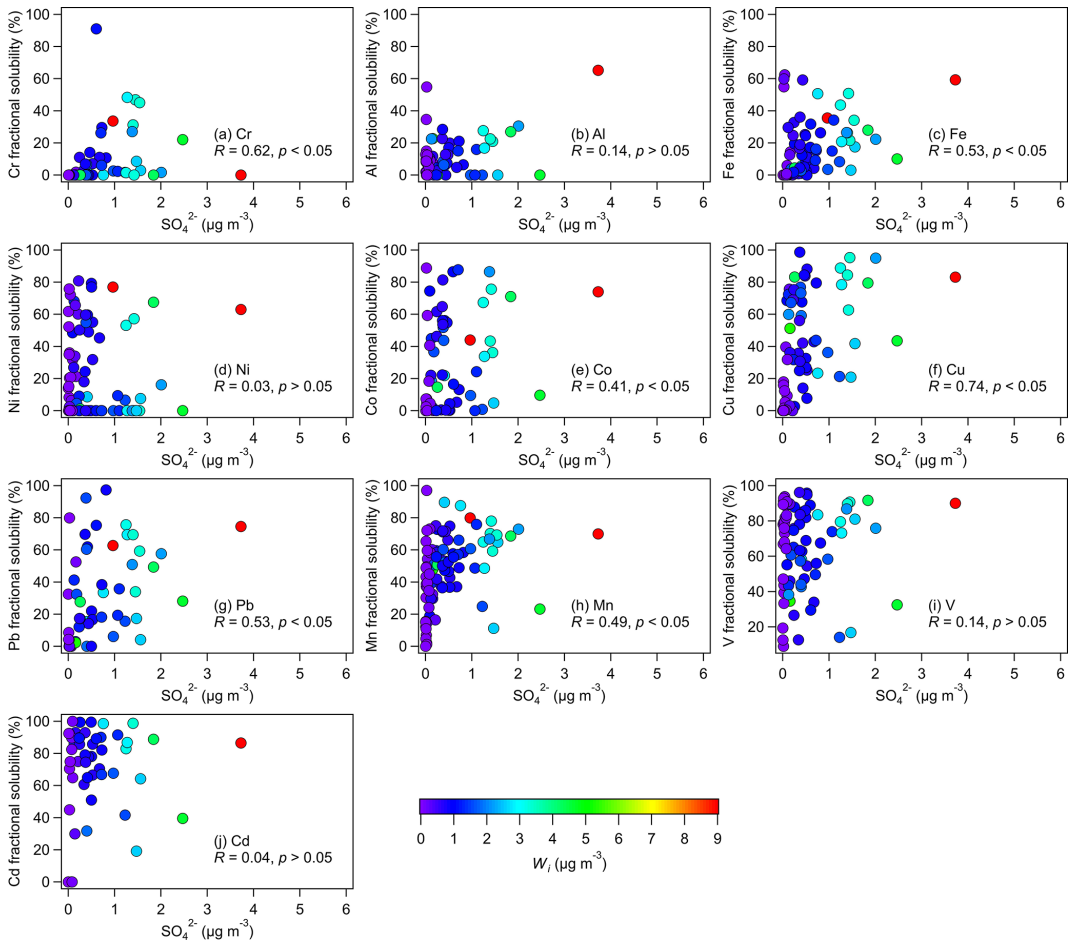

Figure 6. Relationships between the metal fractional solubilities and sulfate mass concentration in fine aerosols. Only data with nonzero total metal concentrations were used in the figures. Also shown are the Spearman correlation coefficients for each relationship. The symbols are colored by the corresponding W_i concentrations calculated by ISORROPIA II. The W_i concentrations increased with sulfate concentrations.

Cd fractional solubilities were weak and not statistically significant. Interestingly, the V and Cd fractional solubilities showed weak correlations with the sulfate concentration ($R = 0.14$ and $R = 0.04$, respectively), whereas their water-soluble concentrations showed strong correlations with the sulfate concentration ($R = 0.65$ and $R = 0.74$, respectively). It is possible that the strong correlations of sulfate concentration with water-soluble V and Cd concentrations but not with V and Cd fractional solubilities were due to a large fraction of water-soluble V and Cd having the same sources as sulfate and its precursor (i.e., SO_2). For instance, Celo et al. (2015) reported that substantial concentrations of water-soluble aerosol metals (including V), sulfate, and SO_2 are present in exhaust emissions from the main engines of commercial marine vessels.

High levels of aerosol acidity and liquid water are generally needed for the acid dissolution of metals in an aqueous aerosol particle. In addition to being the main contributor to aerosol acidity levels (i.e., H^+_{air}), sulfate is a highly hygroscopic species that will influence the overall aerosol water uptake behavior, which will drive W_i. Sulfate was the main driver of W_i in fine aerosols in our study, as the mass concentrations of nitrate (another highly hygroscopic species) were very low (about 18 times lower than sulfate, on average). Both W_i and H^+_{air} were controlled primarily by sulfate (sulfate and W_i: $R = 0.90$, $p < 0.05$; sulfate and H^+_{air}: $R = 0.63$, $p < 0.05$). Thus, we analyzed the relationships between the aerosol metal fractional solubilities and W_i and H^+_{air} (Figs. S7, S8). Table 1 shows that correlations between the Al, Ni, V, and Cd fractional solubilities and W_i and H^+_{air} were weak. Together, the weak correlations between the fractional solubilities of Al, Ni, V, and Cd and sulfate, W_i, and H^+_{air} implied that acid processing may have played a minor role in enhancing the solubilities of these four metals. Other atmospheric processes beyond acid processing (e.g., cloud processing, photoreduction) could have played more important roles in enhancing the solubilities of these four metals (Zhu et al., 1993; Spokes et al., 1994; Kuma et al., 1995). It is possible that these four metals had slow acid dissolution rates as a result of their mineralogy and oxida-

tion states. The impacts of mineralogy and oxidation states on the susceptibilities of water-insoluble Al, Ni, V, and Cd to acid dissolution are currently not known. However, previous studies have shown that different aerosol Fe mineralogy and oxidation states have different susceptibilities to acid dissolution that will occur at different timescales (Ingall et al., 2018). Hence, analogous to Fe, it is possible that the mineralogy and oxidation states of Al, Ni, V, and Cd in the collected aerosols may have resulted in these four metals being less susceptible to acid processing, which in turn caused them to undergo slow sulfate-driven acid dissolution from water-insoluble forms to water-soluble forms.

Table 1 shows that the Cr, Fe, Co, Cu, Pb, and Mn fractional solubilities were positively correlated with W_i and H^+_{air}, and these correlations were statistically significant. Together, the statistically significant positive correlations between the fractional solubilities of Cr, Fe, Co, Cu, Pb, and Mn and sulfate, W_i, and H^+_{air} indicated that acid processing likely played an important role in enhancing the solubilities of these six metals. The fractional solubilities of Co, Cu, Pb, and Mn were more strongly correlated with the W_i concentration than with the H^+_{air} concentration. This suggested that W_i had a stronger influence on the acid dissolution of Co, Cu, Pb, and Mn. The strong influence that W_i has on the metal fractional solubility could be explained by the role of aerosol water as a reaction medium for the acid dissolution of metals in an aqueous aerosol particle. Wong et al. (2020) previously showed that, at a relatively constant aerosol pH, a decrease in W_i will lead to a decrease in the reaction medium volume, which in turn will lead to decreases in the overall formation rates of water-soluble metals. Conversely, the fractional solubilities of Cr and Fe were more strongly correlated with the H^+_{air} concentration than with the W_i concentration. This suggested that the aerosol acidity levels had a stronger influence on the acid dissolution of Cr and Fe. Despite the statistically significant positive correlations between the fractional solubilities of Cr, Fe, Co, Cu, Pb, and Mn and sulfate, W_i, and H^+_{air} (Table 1), there was significant scatter in the datasets (Figs. 6, S7, S8). This scatter could be a result of the sulfate, W_i, H^+_{air}, and total and water-soluble metal concentrations being substantially different in individual aerosol particles, which would not be captured by the bulk chemical analysis and thermodynamic modeling performed in this study. The metal dissolution rates in individual aerosol particles could also be significantly different due to differences in metal mineralogy, aerosol acidity levels, etc. in individual aerosol particles. In addition, a recent study by Yang et al. (2021) reported that the filterable metal fractions in the water extracts may contain some metals in water-insoluble forms with small diameters that allowed them to pass through the pores of syringe filters. This would result in overestimated metal fractional solubilities, which could explain why some of the data points in Fig. 6 showed high metal fractional solubilities at low sulfate concentrations.

Interestingly, variability in the aerosol pH did not appear to be a key driver of the variability in the solubilities of Cr, Fe, Co, Cu, Pb, and Mn. It was difficult to discern aerosol pH-dependent fractional solubility trends for these six metals, and their fractional solubilities were not highly correlated with aerosol pH (Table 1, Fig. S9). This could be attributed partly to the scatter in the datasets caused by differences in the metal solubilities and pH in individual aerosol particles that would not be captured by the bulk chemical analysis and thermodynamic modeling performed in this study. The absence of obvious aerosol pH-dependent fractional solubility trends could also be due to the insensitivity of aerosol pH to the variability in sulfate ($R = -0.22$, $p < 0.05$). Based on Eq. (1), the aerosol pH could be viewed simply as the ratio of H^+_{air} to W_i. Both W_i and H^+_{air} were highly variable in this study, and both were controlled primarily by sulfate. As a result, the ratio of H^+_{air} to W_i, or the aerosol pH, would be fairly insensitive to sulfate, even though it was driven primarily by sulfate. Previous studies have similarly reported weak or absent aerosol pH-dependent metal fractional solubility trends, despite evidence of aerosol metal dissolution being enhanced by acid processing (Shi et al., 2020; Wong et al., 2020).

4 Conclusions

In this study, we investigated the abundance and fractional solubilities of 10 metals (Fe, Cu, Al, V, Cr, Mn, Co, Ni, Cd, and Pb) in size-fractionated aerosols collected at an urban site in Hong Kong. Weekly aerosol samples were collected for a month during different seasons from March 2021 to January 2022. The main objective of this study was to identify the key factors that controlled metal solubilities in fine aerosols, with a focus on aerosol metal dissolution via the acid processing and metal–organic complexation mechanisms. Hence, other aerosol chemical species were measured in addition to the total and water-soluble metals.

Higher mass concentrations of total metals were usually measured during the winter and/or spring seasons. This was likely due to the long-range transport of polluted air masses by northerly prevailing winds from emission sources located in continental areas north of Hong Kong. The total metals could be arranged in the following order based on their abundances: Fe > Al > Cu > Co > Mn > Pb > Cr > Ni > V > Cd. This order of abundance was the same for both fine and coarse aerosols. The major sources of the total metals were sea salt, dust, ship emissions, and industrial activities. Higher mass concentrations of water-soluble metals were also usually measured during the winter and/or spring seasons. With the exception of Cu, the water-soluble metals had higher mass concentrations in fine aerosols than in coarse aerosols. The mass concentrations of water-soluble metals generally correlated with the mass concentrations of total metals, which implied that the water-soluble metals were largely derived from their total metals through atmospheric process-

ing and/or that water-soluble and water-insoluble metals have the same emission sources. The study-averaged metal fractional solubilities spanned a wide range for both fine (7.8 % to 71.2 %) and coarse (0.4 % to 47.9 %) aerosols. With the exception of Cu and Co, the metals exhibited higher fractional solubilities in fine aerosols compared with coarse aerosols. The aerosol size-dependent metal fractional solubility could potentially be attributed to differences in the composition and metal mineralogy which resulted in different metal dissolution rates and/or mechanisms for aerosols of different sizes.

The fine aerosols collected in this study were mostly acidic, with about 60 % of the calculated pH values below 3. The acidic nature of the fine aerosols combined with oxalate (which forms metal–organic complexes easily) not being detected in our aerosol samples suggested that organic ligand-promoted dissolution likely played a minor role in enhancing aerosol metal solubilities. This is because organic ligand-promoted metal dissolution is a slow process, and it plays a minor role in metal dissolution under low-pH conditions. Our analyses showed that sulfate, which is the dominant fine-aerosol acidic species, exhibited statistically significant positive correlations with both the water-soluble concentrations of Cr, Fe, Co, Cu, Pb, and Mn and their fractional solubilities. In addition, sulfate controlled W_i and H^+_{air}, both of which are needed for acid dissolution of metals in an aqueous aerosol particle. The water-soluble concentrations of Cr, Fe, Co, Cu, Pb, and Mn and their fractional solubilities exhibited statistically significant positive correlations with both W_i and H^+_{air}. Together, the statistically significant positive correlations between the fractional solubilities of Cr, Fe, Co, Cu, Pb, and Mn and sulfate, W_i, and H^+_{air} indicated that acid processing likely played an important role in enhancing the solubilities of these six metals. The fractional solubilities of Co, Cu, Pb, and Mn were more strongly correlated with the W_i concentration than with the H^+_{air} concentration, which implied that W_i had a stronger influence on the acid dissolution of these four metals. The fractional solubilities of Cr and Fe were more strongly correlated with the H^+_{air} concentration than with the W_i concentration, which implied that the aerosol acidity levels had a stronger influence on the acid dissolution of these two metals. Conversely, our analyses suggested that acid processing played a minor role in enhancing the solubilities of Al, Ni, V, and Cd. It is possible that the mineralogy and oxidation states of these four metals made them less susceptible to acid processing.

In conclusion, this study highlights the key role that sulfate plays in controlling the solubilities of a host of metals in fine aerosols (in this case, Cr, Fe, Co, Cu, Pb, and Mn). This is mostly due to sulfate's ability to both strongly acidify the aerosol particle and provide the liquid reaction medium needed for the acid dissolution of metals. Although this study was performed at an urban site in Hong Kong, we expect our findings to broadly apply to other urban areas in Hong Kong and South China, where sulfate is the dominant acidic and hygroscopic component in fine aerosols. Results from this study can also provide insights into how the solubilities of different aerosol metals will change with the decrease in sulfate as Hong Kong and other cities in South China transition away from coal combustion as their main energy source to improve local and regional air quality and combat climate change.

Data availability. The data used in this publication are available to the community and can be accessed at https://doi.org/10.5281/zenodo.7013770 (Yang et al., 2022).

Supplement. The supplement related to this article is available online at: https://doi.org/10.5194/acp-23-1403-2023-supplement.

Author contributions. JY and TN designed the study. JY collected the field samples. JY, LM, and WCA performed chemical analysis of the field samples. JY, XH, YM, and TN analyzed the data. JY and TN prepared the manuscript with contributions from all co-authors.

Competing interests. One of the authors is a member of the editorial board of *Atmospheric Chemistry and Physics*. The peer-review process was guided by an independent editor, and the authors also have no other competing interests to declare.

Disclaimer. Publisher's note: Copernicus Publications remains neutral with regard to jurisdictional claims in published maps and institutional affiliations.

Financial support. This research has been supported by the Research Grants Council, University Grants Committee (grant no. 21304919).

Review statement. This paper was edited by Amos Tai and reviewed by Mingjin Tang, Akinori Ito, and one anonymous referee.

References

Adachi, K. and Tainosho, Y.: Characterization of heavy metal particles embedded in tire dust, Environ. Int., 30, 1009–1017, https://doi.org/10.1016/j.envint.2004.04.004, 2004.

Al-Abadleh, H. A.: Review of the bulk and surface chemistry of iron in atmospherically relevant systems containing humic-like substances, RSC Adv., 5, 45785–45811, https://doi.org/10.1039/c5ra03132j, 2015.

Al-Abadleh, H. A.: Aging of atmospheric aerosols and the role of iron in catalyzing brown carbon formation, Environ. Sci.-Atmos., 1, 297–345, https://doi.org/10.1039/D1EA00038A, 2021.

Baker, A. R. and Jickells, T. D.: Mineral particle size as a control on aerosol iron solubility, Geophys. Res. Lett., 33, L17608, https://doi.org/10.1029/2006GL026557, 2006.

Baker, A. R., Jickells, T. D., Witt, M., and Linge, K. L.: Trends in the solubility of iron, aluminium, manganese and phosphorus in aerosol collected over the Atlantic Ocean, Mar. Chem., 98, 43–58, https://doi.org/10.1016/j.marchem.2005.06.004, 2006.

Baker, A. R., Li, M., and Chance, R.: Trace Metal Fractional Solubility in Size-Segregated Aerosols From the Tropical Eastern Atlantic Ocean, Global Biogeochem. Cy., 34, e2019GB006510, https://doi.org/10.1029/2019GB006510, 2020.

Bates, J. T., Fang, T., Verma, V., Zeng, L. H., Weber, R. J., Tolbert, P. E., Abrams, J. Y., Sarnat, S. E., Klein, M., Mulholland, J. A., and Russell, A. G.: Review of Acellular Assays of Ambient Particulate Matter Oxidative Potential: Methods and Relationships with Composition, Sources, and Health Effects, Environ. Sci. Technol,, 53, 4003–4019, https://doi.org/10.1021/acs.est.8b03430, 2019.

Birmili, W., Allen, A. G., Bary, F., and Harrison, R. M.: Trace Metal Concentrations and Water Solubility in Size-Fractionated Atmospheric Particles and Influence of Road Traffic, Environ. Sci. Technol., 40, 1144–1153, https://doi.org/10.1021/es0486925, 2006.

Boyd, P. W., Jickells, T., Law, C. S., Blain, S., Boyle, E. A., Buesseler, K. O., Coale, K. H., Cullen, J. J., de Baar, H. J. W., Follows, M., Harvey, M., Lancelot, C., Levasseur, M., Owens, N. P. J., Pollard, R., Rivkin, R. B., Sarmiento, J., Schoemann, V., Smetacek, V., Takeda, S., Tsuda, A., Turner, S., and Watson, A. J.: Mesoscale iron enrichment experiments 1993–2005: Synthesis and future directions, Science, 315, 612–617, https://doi.org/10.1126/science.1131669, 2007.

Bresgen, N. and Eckl, P. M.: Oxidative stress and the homeodynamics of iron metabolism, Biomolecules, 5, 808–847, https://doi.org/10.3390/biom5020808, 2015.

Brook, R. D., Rajagopalan, S., Pope, C. A., Brook, J. R., Bhatnagar, A., Diez-Roux, A. V., Holguin, F., Hong, Y. L., Luepker, R. V., Mittleman, M. A., Peters, A., Siscovick, D., Smith, S. C., Whitsel, L., Kaufman, J. D., Amer Heart Assoc Council, E., Council Kidney Cardiovasc, D., and Council Nutr Phys Activity, M.: Particulate Matter Air Pollution and Cardiovascular Disease An Update to the Scientific Statement From the American Heart Association, Circulation, 121, 2331–2378, https://doi.org/10.1161/CIR.0b013e3181dbece1, 2010.

Celo, V., Dabek-Zlotorzynska, E., and McCurdy, M.: Chemical Characterization of Exhaust Emissions from Selected Canadian Marine Vessels: The Case of Trace Metals and Lanthanoids, Environ. Sci. Technol., 49, 5220–5226, https://doi.org/10.1021/acs.est.5b00127, 2015.

Chen, H. H. and Grassian, V. H.: Iron Dissolution of Dust Source Materials during Simulated Acidic Processing: The Effect of Sulfuric, Acetic, and Oxalic Acids, Environ. Sci. Technol., 47, 10312–10321, https://doi.org/10.1021/es401285s, 2013.

Cheng, Y., Lee, S. C., Cao, J., Ho, K. F., Chow, J., Watson, J., and Ao, C.: Elemental composition of airborne aerosols at a traffic site and a suburban site in Hong Kong, Int. J. Environ. Pollut., 36, 166–179, 2009.

Chow, W. S., Huang, X. H. H., Leung, K. F., Huang, L., Wu, X., and Yu, J. Z.: Molecular and elemental marker-based source apportionment of fine particulate matter at six sites in Hong Kong, China, Sci. Total Environ., 813, 152652, https://doi.org/10.1016/j.scitotenv.2021.152652, 2022.

Chu, B., Hao, J., Li, J., Takekawa, H., Wang, K., and Jiang, J.: Effects of two transition metal sulfate salts on secondary organic aerosol formation in toluene/NOxphotooxidation, Front. Environ. Sci. Eng. 7, 1–9, https://doi.org/10.1007/s11783-012-0476-x, 2013.

Chu, B., Liggio, J., Liu, Y., He, H., Takekawa, H., Li, S.-M., and Hao, J.: Influence of metal-mediated aerosol-phase oxidation on secondary organic aerosol formation from the ozonolysis and OH-oxidation of α-pinene, Scient. Rep., 7, 40311, https://doi.org/10.1038/srep40311, 2017.

Cohen, A. J., Brauer, M., Burnett, R., Anderson, H. R., Frostad, J., Estep, K., Balakrishnan, K., Brunekreef, B., Dandona, L., Dandona, R., Feigin, V., Freedman, G., Hubbell, B., Jobling, A., Kan, H., Knibbs, L., Liu, Y., Martin, R., Morawska, L., Pope, C. A., Shin, H., Straif, K., Shaddick, G., Thomas, M., van Dingenen, R., van Donkelaar, A., Vos, T., Murray, C. J. L., and Forouzanfar, M. H.: Estimates and 25-year trends of the global burden of disease attributable to ambient air pollution: an analysis of data from the Global Burden of Diseases Study 2015, Lancet, 389, 1907–1918, https://doi.org/10.1016/s0140-6736(17)30505-6, 2017.

Costa, D. L. and Dreher, K. L.: Bioavailable transition metals in particulate matter mediate cardiopulmonary injury in healthy and compromised animal models, Environ. Health Perspect., 105, 1053–1060, https://doi.org/10.2307/3433509, 1997.

de Baar, H. J. W., Boyd, P. W., Coale, K. H., Landry, M. R., Tsuda, A., Assmy, P., Bakker, D. C. E., Bozec, Y., Barber, R. T., Brzezinski, M. A., Buesseler, K. O., Boye, M., Croot, P. L., Gervais, F., Gorbunov, M. Y., Harrison, P. J., Hiscock, W. T., Laan, P., Lancelot, C., Law, C. S., Levasseur, M., Marchetti, A., Millero, F. J., Nishioka, J., Nojiri, Y., van Oijen, T., Riebesell, U., Rijkenberg, M. J. A., Saito, H., Takeda, S., Timmermans, K. R., Veldhuis, M. J. W., Waite, A. M., and Wong, C. S.: Synthesis of iron fertilization experiments: From the iron age in the age of enlightenment, J. Geophys. Res.-Oceans, 110, C09S16, https://doi.org/10.1029/2004jc002601, 2005.

Deguillaume, L., Leriche, M., Desboeufs, K., Mailhot, G., George, C., and Chaumerliac, N.: Transition Metals in Atmospheric Liquid Phases: Sources, Reactivity, and Sensitive Parameters, Chem. Rev., 105, 3388–3431, https://doi.org/10.1021/cr040649c, 2005.

Fang, T., Guo, H., Verma, V., Peltier, R. E., and Weber, R. J.: $PM_{2.5}$ water-soluble elements in the southeastern United States: automated analytical method development, spatiotemporal distributions, source apportionment, and implications for heath studies, Atmos. Chem. Phys., 15, 11667–11682, https://doi.org/10.5194/acp-15-11667-2015, 2015.

Fang, T., Guo, H., Zeng, L., Verma, V., Nenes, A., and Weber, R. J.: Highly Acidic Ambient Particles, Soluble Metals, and Oxidative Potential: A Link between Sulfate and Aerosol Toxicity, Environ. Sci. Technol., 51, 2611–2620, https://doi.org/10.1021/acs.est.6b06151, 2017.

Fountoukis, C. and Nenes, A.: ISORROPIA II: a computationally efficient thermodynamic equilibrium model for K^+–Ca^{2+}–Mg^{2+}–NH_4^+–Na^+–SO_4^{2-}–NO_3^-–Cl^-–H_2O aerosols, Atmos. Chem. Phys., 7, 4639–4659, https://doi.org/10.5194/acp-7-4639-2007, 2007.

Fountoukis, C., Nenes, A., Sullivan, A., Weber, R., Van Reken, T., Fischer, M., Matias, E., Moya, M., Farmer, D., and Cohen,

R. C.: Thermodynamic characterization of Mexico City aerosol during MILAGRO 2006, Atmos. Chem. Phys., 9, 2141–2156, https://doi.org/10.5194/acp-9-2141-2009, 2009.

Frampton, M. W., Ghio, A. J., Samet, J. M., Carson, J. L., Carter, J. D., and Devlin, R. B.: Effects of aqueous extracts of PM10 filters from the Utah Valley on human airway epithelial cells, Am. J. Physiol.-Lung Cell. Molec. Physiol., 277, L960–L967, https://doi.org/10.1152/ajplung.1999.277.5.L960, 1999.

Gao, D., Mulholland, J. A., Russell, A. G., and Weber, R. J.: Characterization of water-insoluble oxidative potential of $PM_{2.5}$ using the dithiothreitol assay, Atmos. Enviro., 224, 117327, https://doi.org/10.1016/j.atmosenv.2020.117327, 2020.

Gao, Y., Marsay, C. M., Yu, S., Fan, S., Mukherjee, P., Buck, C. S., and Landing, W. M.: Particle-Size Variability of Aerosol Iron and Impact on Iron Solubility and Dry Deposition Fluxes to the Arctic Ocean, Sci. Rep., 9, 16653, https://doi.org/10.1038/s41598-019-52468-z, 2019.

Gao, Y., Yu, S., Sherrell, R. M., Fan, S., Bu, K., and Anderson, J. R.: Particle-Size Distributions and Solubility of Aerosol Iron Over the Antarctic Peninsula During Austral Summer, J. Geophys. Res.-Atmos., 125, e2019JD032082, https://doi.org/10.1029/2019JD032082, 2020.

Garg, B. D., Cadle, S. H., Mulawa, P. A., Groblicki, P. J., Laroo, C., and Parr, G. A.: Brake Wear Particulate Matter Emissions, Environ. Sci. Technol., 34, 4463–4469, https://doi.org/10.1021/es001108h, 2000.

Garrett, R. G.: Natural Sources of Metals to the Environment, Human Ecol. Risk Assess., 6, 945–963, https://doi.org/10.1080/10807030091124383, 2000.

Giorio, C., D'Aronco, S., Di Marco, V., Badocco, D., Battaglia, F., Soldà, L., Pastore, P., and Tapparo, A.: Emerging investigator series: aqueous-phase processing of atmospheric aerosol influences dissolution kinetics of metal ions in an urban background site in the Po Valley, Environ. Sci.-Process. Impact., 24, 884–897, https://doi.org/10.1039/D2EM00023G, 2022.

He, X., Liu, P., Zhao, W., Xu, H., Zhang, R., and Shen, Z.: Size distribution of water-soluble metals in atmospheric particles in Xi'an, China: Seasonal variations, bioavailability, and health risk assessment, Atmos. Pollut. Res., 12, 101090, https://doi.org/10.1016/j.apr.2021.101090, 2021.

Heal, M. R., Elton, R. A., Hibbs, L. R., Agius, R. M., and Beverland, I. J.: A time-series study of the health effects of water-soluble and total-extractable metal content of airborne particulate matter, Occupat. Environ. Med., 66, 636–638, https://doi.org/10.1136/oem.2008.045310, 2009.

Hopke, P. K., Lamb, R. E., and Natusch, D. F. S.: Multielemental characterization of urban roadway dust, Environ. Sci. Technol., 14, 164–172, https://doi.org/10.1021/es60162a006, 1980.

Ingall, E. D., Feng, Y., Longo, A. F., Lai, B., Shelley, R. U., Landing, W. M., Morton, P. L., Nenes, A., Mihalopoulos, N., Violaki, K., Gao, Y., Sahai, S., and Castorina, E.: Enhanced Iron Solubility at Low pH in Global Aerosols, Atmosphere, 9, 201, https://doi.org/10.3390/atmos9050201, 2018.

Jiang, S. Y., Kaul, D. S., Yang, F., Sun, L., and Ning, Z.: Source apportionment and water solubility of metals in size segregated particles in urban environments, Sci. Total Environ., 533, 347–355, https://doi.org/10.1016/j.scitotenv.2015.06.146, 2015.

Jiang, S. Y. N., Yang, F., Chan, K. L., and Ning, Z.: Water solubility of metals in coarse PM and $PM_{2.5}$ in typical urban environment in Hong Kong, Atmos. Pollut. Res., 5, 236–244, https://doi.org/10.5094/APR.2014.029, 2014.

Jordi, A., Basterretxea, G., Tovar-Sanchez, A., Alastuey, A., and Querol, X.: Copper aerosols inhibit phytoplankton growth in the Mediterranean Sea, P. Natl. Acad. Sci. USA, 109, 21246–21249, https://doi.org/10.1073/pnas.1207567110, 2012.

Kuma, K., Nakabayashi, S., and Matsunaga, K.: Photoreduction of Fe(III) by hydroxycarboxylic acids in seawater, Water Res., 29, 1559–1569, https://doi.org/10.1016/0043-1354(94)00289-J, 1995.

Lakey, P. S. J., Berkemeier, T., Tong, H. J., Arangio, A. M., Lucas, K., Poschl, U., and Shiraiwa, M.: Chemical exposure-response relationship between air pollutants and reactive oxygen species in the human respiratory tract, Scient. Rep., 6, 32916, https://doi.org/10.1038/srep32916, 2016.

Lee, C. S. L., Li, X.-D., Zhang, G., Li, J., Ding, A.-J., and Wang, T.: Heavy metals and Pb isotopic composition of aerosols in urban and suburban areas of Hong Kong and Guangzhou, South China—Evidence of the long-range transport of air contaminants, Atmos. Environ., 41, 432–447, https://doi.org/10.1016/j.atmosenv.2006.07.035, 2007.

Li, W., Wang, T., Zhou, S., Lee, S., Huang, Y., Gao, Y., and Wang, W.: Microscopic Observation of Metal-Containing Particles from Chinese Continental Outflow Observed from a Non-Industrial Site, Environ. Sci. Technol., 47, 9124–9131, https://doi.org/10.1021/es400109q, 2013.

Li, W., Xu, L., Liu, X., Zhang, J., Lin, Y., Yao, X., Gao, H., Zhang, D., Chen, J., Wang, W., Harrison, R. M., Zhang, X., Shao, L., Fu, P., Nenes, A., and Shi, Z.: Air pollution–aerosol interactions produce more bioavailable iron for ocean ecosystems, Sci. Adv., 3, e1601749, https://doi.org/10.1126/sciadv.1601749, 2017.

Lippmann, M.: Toxicological and epidemiological studies of cardiovascular effects of ambient air fine particulate matter ($PM_{2.5}$) and its chemical components: Coherence and public health implications, Crit. Rev. Toxicol., 44, 299–347, https://doi.org/10.3109/10408444.2013.861796, 2014.

Longo, A. F., Feng, Y., Lai, B., Landing, W. M., Shelley, R. U., Nenes, A., Mihalopoulos, N., Violaki, K., and Ingall, E. D.: Influence of Atmospheric Processes on the Solubility and Composition of Iron in Saharan Dust, Environ. Sci. Technol., 50, 6912–6920, https://doi.org/10.1021/acs.est.6b02605, 2016.

Lough, G. C., Schauer, J. J., Park, J.-S., Shafer, M. M., DeMinter, J. T., and Weinstein, J. P.: Emissions of Metals Associated with Motor Vehicle Roadways, Environ. Sci. Technol., 39, 826–836, https://doi.org/10.1021/es048715f, 2005.

Mahowald, N. M., Hamilton, D. S., Mackey, K. R. M., Moore, J. K., Baker, A. R., Scanza, R. A., and Zhang, Y.: Aerosol trace metal leaching and impacts on marine microorganisms, Nat. Commun., 9, 2614, https://doi.org/10.1038/s41467-018-04970-7, 2018.

Mao, J., Fan, S., Jacob, D. J., and Travis, K. R.: Radical loss in the atmosphere from Cu–Fe redox coupling in aerosols, Atmos. Chem. Phys., 13, 509–519, https://doi.org/10.5194/acp-13-509-2013, 2013.

Mao, J., Fan, S., and Horowitz, L. W.: Soluble Fe in Aerosols Sustained by Gaseous HO_2 Uptake, Environ. Sci. Technol. Lett., 4, 98–104, https://doi.org/10.1021/acs.estlett.7b00017, 2017.

Nriagu, J. O.: A global assessment of natural sources of atmospheric trace metals, Nature, 338, 47–49, https://doi.org/10.1038/338047a0, 1989.

Oakes, M., Ingall, E. D., Lai, B., Shafer, M. M., Hays, M. D., Liu, Z. G., Russell, A. G., and Weber, R. J.: Iron Solubility Related to Particle Sulfur Content in Source Emission and Ambient Fine Particles, Environ. Sci. Technol., 46, 6637–6644, https://doi.org/10.1021/es300701c, 2012.

Paatero, P.: Least squares formulation of robust non-negative factor analysis, Chemometr. Intel. Labor. Syst., 37, 23–35, https://doi.org/10.1016/S0169-7439(96)00044-5, 1997.

Paatero, P. and Tapper, U.: Positive matrix factorization: A non-negative factor model with optimal utilization of error estimates of data values, Environmetrics, 5, 111–126, https://doi.org/10.1002/env.3170050203, 1994.

Paris, R. and Desboeufs, K. V.: Effect of atmospheric organic complexation on iron-bearing dust solubility, Atmos. Chem. Phys., 13, 4895–4905, https://doi.org/10.5194/acp-13-4895-2013, 2013.

Paris, R., Desboeufs, K. V., and Journet, E.: Variability of dust iron solubility in atmospheric waters: Investigation of the role of oxalate organic complexation, Atmos. Environ., 45, 6510–6517, https://doi.org/10.1016/j.atmosenv.2011.08.068, 2011.

Paytan, A., Mackey, K. R. M., Chen, Y., Lima, I. D., Doney, S. C., Mahowald, N., Labiosa, R., and Postf, A. F.: Toxicity of atmospheric aerosols on marine phytoplankton, P. Natl. Acad. Sci. USA, 106, 4601–4605, https://doi.org/10.1073/pnas.0811486106, 2009.

Phalen, R. F.: The particulate air pollution controversy, Nonlin. Biol. Toxicol. Med., 2, 259–292, https://doi.org/10.1080/15401420490900245, 2004.

Pye, H. O. T., Nenes, A., Alexander, B., Ault, A. P., Barth, M. C., Clegg, S. L., Collett Jr, J. L., Fahey, K. M., Hennigan, C. J., Herrmann, H., Kanakidou, M., Kelly, J. T., Ku, I. T., McNeill, V. F., Riemer, N., Schaefer, T., Shi, G., Tilgner, A., Walker, J. T., Wang, T., Weber, R., Xing, J., Zaveri, R. A., and Zuend, A.: The acidity of atmospheric particles and clouds, Atmos. Chem. Phys., 20, 4809–4888, https://doi.org/10.5194/acp-20-4809-2020, 2020.

Schroth, A. W., Crusius, J., Sholkovitz, E. R., and Bostick, B. C.: Iron solubility driven by speciation in dust sources to the ocean, Nat. Geosci., 2, 337–340, https://doi.org/10.1038/ngeo501, 2009.

Sedwick, P. N., Sholkovitz, E. R., and Church, T. M.: Impact of anthropogenic combustion emissions on the fractional solubility of aerosol iron: Evidence from the Sargasso Sea, Geochem. Geophy. Geosy., 8, Q10Q06, https://doi.org/10.1029/2007GC001586, 2007.

Shelley, R. U., Landing, W. M., Ussher, S. J., Planquette, H., and Sarthou, G.: Regional trends in the fractional solubility of Fe and other metals from North Atlantic aerosols (GEOTRACES cruises GA01 and GA03) following a two-stage leach, Biogeosciences, 15, 2271–2288, https://doi.org/10.5194/bg-15-2271-2018, 2018.

Shi, J., Guan, Y., Ito, A., Gao, H., Yao, X., Baker, A. R., and Zhang, D.: High Production of Soluble Iron Promoted by Aerosol Acidification in Fog, Geophys. Res. Lett., 47, e2019GL086124, https://doi.org/10.1029/2019GL086124, 2020.

Sholkovitz, E. R., Sedwick, P. N., Church, T. M., Baker, A. R., and Powell, C. F.: Fractional solubility of aerosol iron: Synthesis of a global-scale data set, Geochim. Cosmochim. Ac., 89, 173–189, https://doi.org/10.1016/j.gca.2012.04.022, 2012.

Slikboer, S., Grandy, L., Blair, S. L., Nizkorodov, S. A., Smith, R. W., and Al-Abadleh, H. A.: Formation of Light Absorbing Soluble Secondary Organics and Insoluble Polymeric Particles from the Dark Reaction of Catechol and Guaiacol with Fe(III), Environ. Sci. Technol., 49, 7793–7801, https://doi.org/10.1021/acs.est.5b01032, 2015.

Spokes, L. J., Jickells, T. D., and Lim, B.: Solubilisation of aerosol trace metals by cloud processing: A laboratory study, Geochim. Cosmochim. Ac., 58, 3281–3287, https://doi.org/10.1016/0016-7037(94)90056-6, 1994.

Tao, Y. and Murphy, J. G.: The Mechanisms Responsible for the Interactions among Oxalate, pH, and Fe Dissolution in $PM_{2.5}$, ACS Earth Space Chem., 3, 2259–2265, https://doi.org/10.1021/acsearthspacechem.9b00172, 2019.

Wang, W., Liu, M., Wang, T., Song, Y., Zhou, L., Cao, J., Hu, J., Tang, G., Chen, Z., Li, Z., Xu, Z., Peng, C., Lian, C., Chen, Y., Pan, Y., Zhang, Y., Sun, Y., Li, W., Zhu, T., Tian, H., and Ge, M.: Sulfate formation is dominated by manganese-catalyzed oxidation of SO_2 on aerosol surfaces during haze events, Nat. Commun., 12, 1993, https://doi.org/10.1038/s41467-021-22091-6, 2021.

Wang, Z. Z., Fu, H. B., Zhang, L. W., Song, W. H., and Chen, J. M.: Ligand-Promoted Photoreductive Dissolution of Goethite by Atmospheric Low-Molecular Dicarboxylates, J. Phys. Chem. A, 121, 1648–1657, https://doi.org/10.1021/acs.jpca.6b09160, 2017.

Wong, J. P. S., Yang, Y., Fang, T., Mulholland, J. A., Russell, A. G., Ebelt, S., Nenes, A., and Weber, R. J.: Fine Particle Iron in Soils and Road Dust Is Modulated by Coal-Fired Power Plant Sulfur, Environ. Sci. Technol., 54, 7088–7096, https://doi.org/10.1021/acs.est.0c00483, 2020.

Yang, Y., Gao, D., and Weber, R. J.: A method for liquid spectrophotometric measurement of total and water-soluble iron and copper in ambient aerosols, Atmos. Meas. Tech., 14, 4707–4719, https://doi.org/10.5194/amt-14-4707-2021, 2021.

Yang, Y., Ma, L., He, X., Au, W. C., Miao, Y., Wang, W. X., and Nah, T.: Abundance and fractional solubilities of aerosol metals in urban Hong Kong: Insights into factors that control aerosol metal dissolution in an urban site in South China, Zenodo [data set], https://doi.org/10.5281/zenodo.7013770, 2022.

Ye, D., Klein, M., Mulholland, J. A., Russell, A. G., Weber, R., Edgerton, E. S., Chang, H. H., Sarnat, J. A., Tolbert, P. E., and Ebelt Sarnat, S.: Estimating Acute Cardiovascular Effects of Ambient $PM_{2.5}$ Metals, Environ. Health Perspect., 126, 027007, https://doi.org/10.1289/ehp2182, 2018.

Zhang, H., Li, R., Dong, S., Wang, F., Zhu, Y., Meng, H., Huang, C., Ren, Y., Wang, X., Hu, X., Li, T., Peng, C., Zhang, G., Xue, L., Wang, X., and Tang, M.: Abundance and Fractional Solubility of Aerosol Iron During Winter at a Coastal City in Northern China: Similarities and Contrasts Between Fine and Coarse Particles, J. Geophys. Res.-Atmos., 127, e2021JD036070, https://doi.org/10.1029/2021JD036070, 2022.

Zhao, Z., Luo, X. S., Jing, Y. S., Li, H. B., Pang, Y. T., Wu, L. C., Chen, Q., and Jin, L.: In vitro assessments of bioaccessibility and bioavailability of $PM_{2.5}$ trace metals in respiratory and digestive systems and their oxidative potential, J. Hazard. Mater., 409, 124638, https://doi.org/10.1016/j.jhazmat.2020.124638, 2021.

Zhong, L., Louie, P. K. K., Zheng, J., Yuan, Z., Yue, D., Ho, J. W. K., and Lau, A. K. H.: Science–policy inter-

play: Air quality management in the Pearl River Delta region and Hong Kong, Atmos. Environ., 76, 3–10, https://doi.org/10.1016/j.atmosenv.2013.03.012, 2013.

Zhou, Y., Zhang, Y., Griffith, S. M., Wu, G., Li, L., Zhao, Y., Li, M., Zhou, Z., and Yu, J. Z.: Field Evidence of Fe-Mediated Photochemical Degradation of Oxalate and Subsequent Sulfate Formation Observed by Single Particle Mass Spectrometry, Environ. Sci. Technol., 54, 6562–6574, https://doi.org/10.1021/acs.est.0c00443, 2020.

Zhu, X., Prospero, J. M., Savoie, D. L., Millero, F. J., Zika, R. G., and Saltzman, E. S.: Photoreduction of iron(III) in marine mineral aerosol solutions, J. Geophys. Res. Atmos., 98, 9039–9046, https://doi.org/10.1029/93JD00202, 1993.

Zhu, Y., Li, W., Lin, Q., Yuan, Q., Liu, L., Zhang, J., Zhang, Y., Shao, L., Niu, H., Yang, S., and Shi, Z.: Iron solubility in fine particles associated with secondary acidic aerosols in east China, Environ. Pollut., 264, 114769, https://doi.org/10.1016/j.envpol.2020.114769, 2020.